

# An Online Fuel Consumption and Emission Reduction Power Management Strategy for Plug-in Hybrid Electric Vehicles

Hasan Alipour<sup>\*1</sup>, Behzad Asaei<sup>2</sup>

School of Electrical and Computer Engineering, college of Engineering, University of Tehran, Tehran, Iran

<sup>\*1</sup>hasan.alipour2006@gmail.com; <sup>2</sup> basaei@ut.ac.ir

## Abstract

An online power management strategy (PMS) for plug-in hybrid electric vehicles is presented in this paper. This PMS with the capability to reduce both the fuel consumption and the emission, has simple mathematics and excludes a priori knowledge of the driving cycle. The only required information is the driving duration that can be estimated by the driver or by the vehicle information systems, so the proposed method can be easily implemented. Furthermore, an adaptive form of this PMS is presented and its performance is compared with other strategies. Using the online adaptive PMS method, the incoming driving cycle condition is predicted by the vehicle past conditions. In this paper, the engine fuel characteristics are linearized to several zones. At any instant, one of these zones is selected for the engine operation. In each zone, an optimal cost function is minimized for the fuel consumption and the emission reduction. Moreover, different cost functions are defined and used on various engines. Finally, the proposed PMS is simulated in the ADVISOR environment and compared with conventional method.

## Keywords

*Adaptive Control; Fuel Consumption and Emission Reduction; Plug-in Hybrid Electric Vehicle; Power Management Strategy*

## Introduction

Increasing fossil fuel consumption has caused significant problems for both governments and societies. These non-renewable resources are depleting very fast. Furthermore, the air pollution and the greenhouse effects of their emissions, damage the general health. Since a big share of the fuel consumption is used by the conventional vehicles, the hybrid electric vehicles (HEVs) are suggested as an effective solution to reduce the fuel consumption. In HEVs, an electric power source is integrated into a conventional internal combustion engine which is downsized. However, the main source of their traction power is still the gasoline engine. The hybridization

and downsizing allow for fuel economy enhancements (Katrasnik et al., 2007). Thanks to the presence of an electric power train, these vehicles have the regenerative braking ability that increases the vehicle efficiency (Yu-shan Li et al., 2009).

The latest generation of the HEVs is the Plug-in hybrid electric vehicles (PHEVs) that employ the grid electric energy. For example, they can be plugged into a power grid or a residential photovoltaic system (Gurkaynak et al., 2009). The PHEVs consume 40% to 80% fuel than conventional HEVs (Fajri et al., 2008).

IEEE-USA Energy Policy Committee defines that a PHEV should have at least a 4 kWh battery storage system and ten miles only electric mode driving distance (Shams-Zahraei et al., 2009). Therefore, the PHEVs have a medium storage system that is charged externally. Usually, the electric energy is cheaper than the gasoline (four times in USA (Romm et al., 2006)). Therefore, it is essential to use the stored energy before the end of the trip that makes the PMS more complicated. The PMS defines the component's power share. Many PMSs are proposed and classified into the HEVs and the PHEVs. From the mathematical point of view, the PMSs are classified into rule based and optimization based methods (Bayindir et al. 2011; Wirasingha et al. 2011).

There are many heuristic and fuzzy rule based PMSs in recent literatures (Gao et al., 2010; Hui et al., 2008; Banvait et al., 2009; Mapelli et al., 2009; Li et al., 2010; Chen Zheng et al., 2009; Xiong et al. 2009). A novel rule-based PMS for the PHEVs that focuses on all electric range and charge depletion range operations is presented in (Gao et al., 2010). An engine on-off rule based control strategy with consideration on position of acceleration pedal is proposed in (Hui et al., 2008). A heuristic solution to a parallel and series-parallel PHEV is proposed in (Banvait et al., 2009). In this

paper, the energy management optimizes engine operational efficiency while maintaining battery state of charge. A rule based fuzzy logic control strategy for a parallel hybrid electric city public bus is proposed in (Li et al., 2010). A series-parallel structure for a hybrid electric bus is presented in (Xiong et al. 2009). In this paper, a fuzzy logic PMS, which consists of two fuzzy modules used to determine the operation mode and distribute torques at parallel mode respectively, is studied by numerical simulation. However, the emission reduction is exclusive of consideration in (Xiong et al. 2009). The rule based PMSs are simple, applicable, and can be calculated easily. However, the optimization based PMSs are usually more efficient than the rule based PMSs (Bayindir et al., 2011; Wirasingha et al. 2011).

Generally, the optimization based PMSs are more complicated and accurate than the rule based PMSs and for both, a priori knowledge about the driving cycle is essential. This essential priori knowledge can be delivered by the solutions provided in literatures. However, they can lead to some more additional computational burden. Therefore, these PMSs are unsuitable for the real applications. The optimization methods define and minimize a cost function (Wirasingha et al. 2011). Both of the fuel consumption and the emission production are minimized easily by means of the proper cost function definition. The optimization group includes a wide spectrum of different methods such as the static optimization, numerical optimization, equivalent consumption minimization strategy (ECMS) and analytical optimization methods (Sciarretta et al., 2007).

One of the interesting optimization PMS is dynamic programming (DP) (Shen et al., 2010; Yan et al., 2010). DP is significant time consuming with heavy mathematical burden. Therefore, a two-scale DP is proposed to solve the mentioned problems (Gong et al., 2007; Gong et al. 2008; Gong et al., 2009). Furthermore, the driving cycle prediction can be done by the new geographical systems like GPS, GIS, and traffic information system (Zhang et al., 2010; Abdul-Hak et al., 2009; Gong et al., 2008; Gong et al., 2007). (Moura et al., 2011) uses a stochastic dynamic programming to optimize PHEV power management over a distribution of drive cycles, rather than a single cycle by means of Markov chains. An optimization PMS by using the Pontryagin's minimum principle for the PHEVs is proposed in (Stockar et al., 2010). The

equivalent fuel consumption strategies (ECMS) are proposed by (Mapelli et al., 2009; Tulpule et al., 2009; Zhang et al., 2010). An artificial neural networks monitoring and fault diagnosis system for electric vehicles is proposed by (Kalogirou et al., 2000) that can be improved for energy management optimization.

This paper presents a PMS that is inspired from (Kessels et al., 2008; Koot et al, 2005), and ECMS method. The presented PMS is designed for the fuel consumption and the emission reduction. The different forms of this PMS and their effects are discussed in this paper.

The proposed PMS is an applicable and accurate method with the simple mathematic equations. Therefore, it has the advantages of the optimization and rule based methods and can be done online. This strategy just needs the driving duration that can be easily estimated by the driver or the geographical and information systems.

This paper is organized as follows: An adequate vehicle model is presented in Section 2. The background of the proposed PMS and its mathematics are discussed in Section 3. The zone selection procedure is discussed in Section 4. In Section 5, an adaptive form of the proposed control strategy is discussed, and the simulation results are presented in Section 6. Finally, conclusions are stated in Section 7.

## Vehicle Model

The focus of this paper is on the parallel PHEV topology. The schematic of this topology is shown in Fig. 1. In this research, the dynamics of the systems with low frequency (lower than one second) are ignored as they have insignificant effects on the fuel consumption of the PHEV. The proposed PMS is simulated in the ADVISOR environment, in which this tool is introduced in (Markel et al., 2002). However, the basic equations of this model are discussed as follows.

### Internal Combustion Engine (ICE)

The fuel consumption and emission rates of an ICE are functions of the engine output power ( $P_m$ ) and the engine speed as (1)-(4):

$$fuel_{rate} = f(P_m, \omega) \quad (1)$$

$$HC_{rate} = hc(P_m, \omega) \quad (2)$$

$$CO_{rate} = co(P_m, \omega) \quad (3)$$

$$NOx_{rate} = nox(P_m, \omega) \quad (4)$$

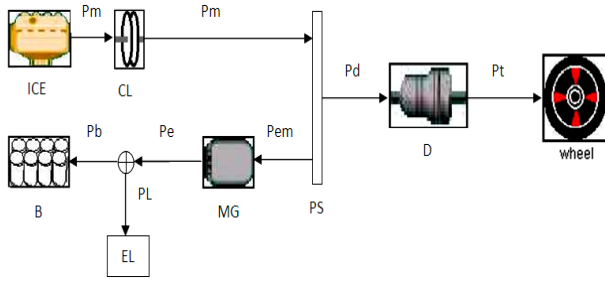


FIG. 1 THE PARALLEL PHEV TOPOLOGY

Where,  $\omega$  is the engine speed and  $P_m$  is the engine power which is a positive parameter. In this paper, HC, CO, and  $NO_x$  are considered as engine emissions.

### Clutch (CL)

The vehicle engine is engaged and disengaged from the drive train by a clutch. The clutch will be disengaged during the shifting time of the gearbox, when the engine is off, and when the speed of the clutch becomes lower than the engine idle speed.

### Motor/Generator (MG)

There is at least one electrical machine in a PHEV that can act as a motor or a generator. Thus, the electric machine is addressed in this paper as motor/generator (MG).

Unlike ICE, the output power of the MG can be positive or negative. In this paper, the sign of  $P_e$  is considered positive when the MG is operated as a generator and negative when it is operated as a motor.

Neglect of friction loss at no load, the MG can be modelled as follows:

$$P_{em} = \max(\eta_{mm} P_e, \frac{1}{\eta_{gm}} P_e) \quad (5)$$

$\eta_{mm}$  and  $\eta_{gm}$  are the efficiency of MG in motor and generator modes, respectively.

$$\eta_{mm} = \frac{P_{em}}{P_e} \quad (6)$$

$$\eta_{gm} = \frac{P_e}{P_{em}} \quad (7)$$

$P_{em}$  is the MG power on the mechanical side and  $P_e$  is that on the electrical side. The defined MG power limits in (8) are applied to the mechanical side.

$$P_{em\_min}(\omega) < P_{em}(\omega) < P_{em\_max}(\omega) \quad (8)$$

### Drive Train (D)

The traction power ( $P_t$ ) is the required wheels power that can be expressed as (9) (Gao et al., 2010).

$$P_t = v(Mgf_r + \frac{1}{2} \rho_a C_D A_f v^2 + M\delta \frac{dv}{dt} + Mgi) \quad (W) \quad (9)$$

where,  $M$  is the vehicle mass;  $v$  is the vehicle speed;  $g$  is the gravity acceleration,  $\rho_a$  is the air mass density;  $C_D$  is the aerodynamic drag coefficient of the vehicle;  $A_f$  is the front area of the vehicle;  $\delta$  is the rotational inertia factor;  $dv/dt$  is the acceleration, and  $i$  is the grade of the road.

If  $P_d$  is regarded as the input power to the drive train, it can be calculated by (10).

$$P_d = \omega_d \times T_d \quad (10)$$

where,  $\omega_d$  and  $T_d$  are the crankshaft speed and torque, respectively.

$$\omega_d = \frac{f_d}{r} v \quad (11)$$

$$T_d = \frac{P_t}{\omega_d \eta_d} \quad (12)$$

where  $f_d$  is the drive train ratio,  $r$  is the wheel radius and  $\eta_d$  is the efficiency of the drive train.

### Power Split (PS)

The power split is assumed to have no energy losses and provides the following power balance:

$$P_m = P_d + P_{em} \quad (13)$$

### Battery (B)

The battery is modelled by a voltage source and a series resistance that represents the battery's internal and terminal losses. Therefore, (14) shows the relation between terminal power ( $P_b$ ) and the net internal power ( $P_s$ ) of the battery.  $\eta^+$  and  $\eta^-$  are the efficiency of the battery during charge and discharge modes, respectively.

$$P_b = \max(\frac{P_s}{\eta^+}, \eta^- P_s) \quad (14)$$

The battery storage energy ( $E_s$ ) is calculated as:

$$E_s(t) = E_s(0) + \int_0^t P_s(t) dt \quad (15)$$

The SOE of the battery is defined as the percentage of the remained energy in the battery to the total theoretical energy capacity of that ( $E_{cap}$ ).

$$SOE(t) = \frac{E_s(t)}{E_{cap}} \times 100 \quad [\%] \quad (16)$$

If the battery open clamp voltage is considered almost constant, the battery state of charge (SOC) can be regared equal to  $SOE$ .

### Electric Load (EL)

Electric load (EL) represents auxiliaries such as head lights, radio, etc. The power consumed by EL is called PL. For simplicity, this power is assumed to be constant and equal to 700 W.

### Problem Definition

It is expected that PMS maintain the vehicle performance and at the same time reduce the fuel consumption and emission. The strategy should be practical and easily applicable on the vehicle. Furthermore, the PMS should be causal. However, some predictive control strategies have been developed with some priori knowledge, but it can lead to some additional computational burden. The presented PMS has a little dependence on a priori information. Essential priori information for the proposed PMS is just the driving duration that can be estimated by the assumption on the constant acceleration and deceleration rate as well as the speed limits for each road (Gong et al., 2007; Gong et al., 2008). The proposed PMS with simple mathematics can be supported by common processors. Therefore, the presented PMS is practical and can be applied easily to the vehicle.

The proposed PMS is inspired from the concepts of the rule based, and the optimization based strategies. Consequently, it has advantages of both.

This strategy is mainly based on ICE characteristics. In the vehicles, the ICE consumes fuel and produces pollution. Therefore, the proper ICE handling causes the significant emission and fuel consumption reduction. Generally, in many literatures, the engine torque-speed map is considered. However, this study is established base on the fuel consumption characteristics.

The fuel consumption characteristics for SI41 and Prius ADVISOR engine models are shown in Fig. 2 and Fig. 3, in which the curves are related to different engine speeds. Each curve is linearized and discretized into several zones that limit the engine operation. In this paper, each curve is divided into 11 zones. The SI41 has a very rugged fuel characteristic, whereas the

fuel characteristic of Prius is monotonous. In other words, the slope of the Prius curves decreases with the increase of power. The Prius engine special structure results from this monotonous characteristic. The Prius engine torque-speed map is shown in Fig. 4 in which that at a constant speed, the engine efficiency increases due to the rise in torque causes. However, the most efficient area of common engines is usually in the areas lower than the maximum torque. For instance, the torque-speed map of the SI41 engine which is a common engine is shown in Fig. 5.

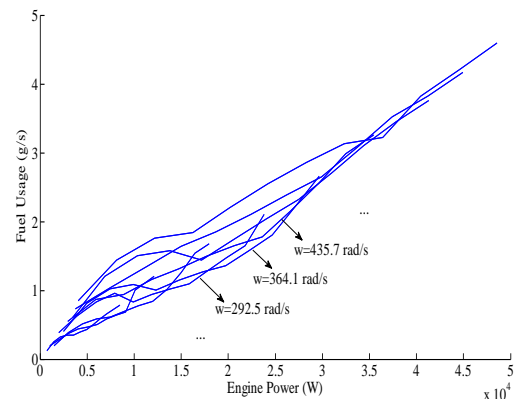


FIG. 2 FUEL MAP CHARACTERISTIC FOR THE SI41 ENGINE

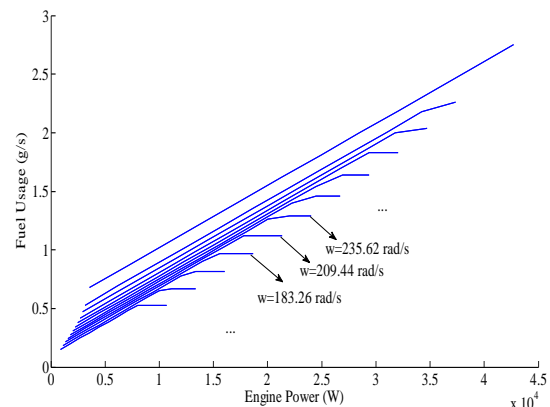


FIG. 3 FUEL MAP CHARACTERISTIC FOR THE PRIUS ENGINE

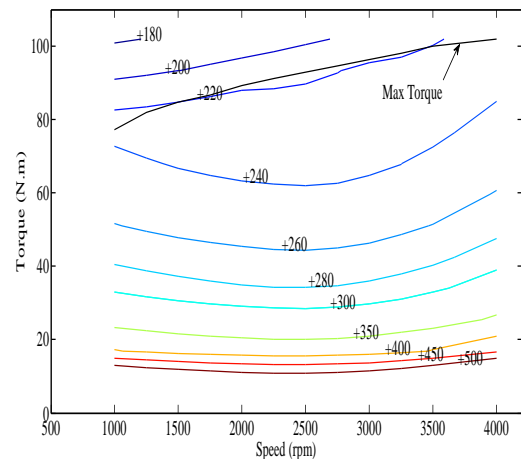


FIG. 4 PRIUS FUEL CONSUMPTION MAP IN GRAM PER KWH

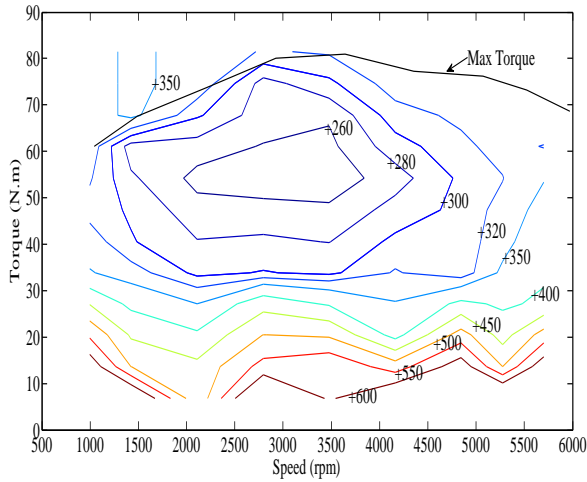


FIG. 5 SI41 FUEL CONSUMPTION MAP IN GRAM PER KWH

A power management strategy for HEVs is presented in (Kessels et al., 2008). The idea of (Kessels et al., 2008) is that the engine should work in the area with high (or low dependence on the engine map) slope when the SOC of the battery is low and work in the area with low (or high) slope when the SOC is high. Therefore, PMS can be compatible for engines like the Prius, but it is unsuitable for engines with a rugged fuel map like SI41.

Fig. 2 and Fig. 3 show that the fuel consumption decreases if the engine speed descends with constant power. Therefore, in series PHEVs or in the topologies that the speed of the engine is controllable; the engine operation at low speeds will be suitable.

The slope of each zone is an important parameter of the proposed PMS. Typically, the slope of each zone ( $\lambda_{fi}$ ) is constant, where  $i$  indicates the zone number.  $\lambda_{fi}$  represents the extra fuel mass flow needed to produce a small amount of mechanical power by the engine.

$$\lambda_{fi}(P_m, \omega) = \frac{\partial f(P_m, \omega)}{\partial P_m} \quad (17)$$

The slopes of different zones and curves are calculated and gathered in a lookup table. Furthermore, the similar lookup tables are prepared for emission characteristics. The characteristics of these emissions for SI41 engine are shown in the Figs. 6-8.

The variations of HC and CO against power changes are similar to the fuel usage variations. Consequently, the attempt on fuel reduction causes a reduction of CO and HC emissions. However, the difference between the NO<sub>x</sub> and the fuel characteristics is significant. In fact, there are some zones with high NO<sub>x</sub> emission in

the optimal fuel consumption area. This difference can have important effects on the PMS for NO<sub>x</sub> reduction. Hence, for reduction of the NO<sub>x</sub> emissions, these zones can be avoided. Certainly, the fuel consumption rate is increased, but it is not significant. In fact, the engine operating point is still in the optimal fuel usage area, inside of which there are just some holes. Thus, a suitable balance between fuel usage and NO<sub>x</sub> emission is achieved.

Different engines have various fuel and emission characteristics. Consequently, this strategy performance and its setting will be different from each other. There is more discussion about the effect of engine characteristics on the PMS results in Section 6.

The emission curves should be discretized and linearized same as fuel consumption curves. The slope of each zone of the HC, CO and NO<sub>x</sub> characteristic curves are given in (18)-(20), respectively.

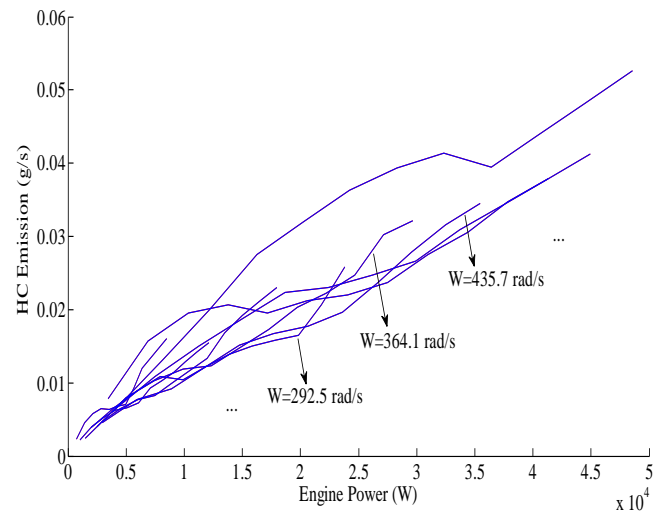


FIG. 6 HC EMISSION MAP CHARACTERISTIC FOR SI41 ENGINE

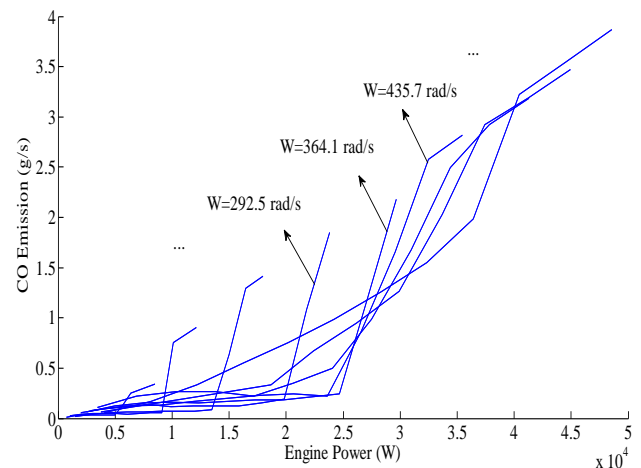


FIG. 7 CO EMISSION MAP CHARACTERISTIC FOR SI41 ENGINE

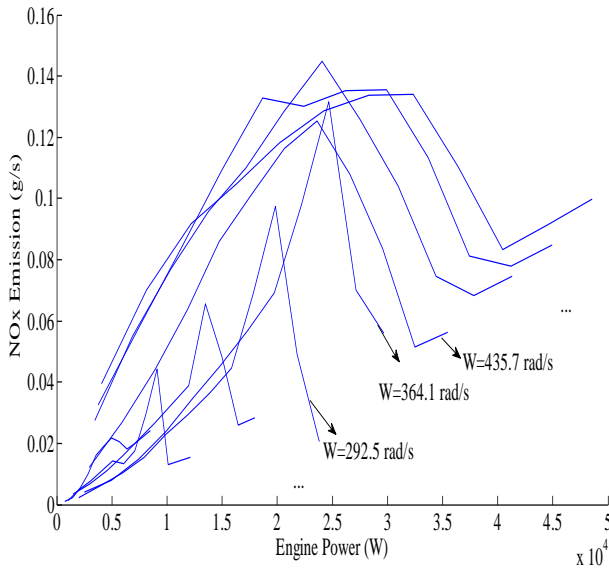


FIG. 8 NO<sub>x</sub> EMISSION MAP CHARACTERISTIC FOR SI41 ENGINE

$$\lambda_{hci}(P_m, \omega) = \frac{\partial hc(P_m, \omega)}{\partial P_m} \quad (18)$$

$$\lambda_{coi}(P_m, \omega) = \frac{\partial co(P_m, \omega)}{\partial P_m} \quad (19)$$

$$\lambda_{noxi}(P_m, \omega) = \frac{\partial nox(P_m, \omega)}{\partial P_m} \quad (20)$$

Thus, (1)-(4) can be linearized as follows:

$$f_i(P_m, \omega) \approx f_{0i}(\omega) + \lambda_{fi}(P_m, \omega) \cdot P_m \quad (21)$$

$$hc_i(P_m, \omega) \approx hc_{0i}(\omega) + \lambda_{hci}(P_m, \omega) \cdot P_m \quad (22)$$

$$co_i(P_m, \omega) \approx co_{0i}(\omega) + \lambda_{coi}(P_m, \omega) \cdot P_m \quad (23)$$

$$nox_i(P_m, \omega) \approx nox_{0i}(\omega) + \lambda_{noxi}(P_m, \omega) \cdot P_m \quad (24)$$

$i = 1, 2, \dots, N_f$

where  $f_{0i}$ ,  $hc_{0i}$ ,  $co_{0i}$ , and  $nox_{0i}$  indicate the initial fuel usage and emission rates of the HC, CO, and NO<sub>x</sub> for the  $i$ -th zone, respectively, and  $N_f$  is the number of the zones.

By the selection of the proper zone, the approximate fuel consumption and emission can be calculated. In order to find this zone, it is required to find the optimal value of  $\lambda_f$  that is explained in more details in Section 4. Then by solving an instantaneous optimal cost function, an appropriate power share value for the ICE and MG is calculated. This instantaneous optimal cost function is derived from the cost function of the ECMS method, in which an instantaneous cost function is defined for equivalent fuel minimization

(Mapelli et al., 2009). (25) explains this cost function where  $J(t)$  is the equivalent fuel usage,  $f(P_m)$  is the real fuel usage by ICE,  $H_l$  is the low heating value of the fuel, and  $s$  is the equivalent factor that depends on the driving cycle and the efficiency of components of the power train (Zhang et al., 2010).

$$J(t) = f(P_m) - \frac{s}{H_l} P_{em} \quad (25)$$

By linearizing the fuel map, the ratio of the equivalent factor and  $H_l$  is considered equal to the slope of the chosen operation zone ( $\lambda_f$ ). For each zone ( $i$ ), there is a certain slope called  $\lambda_{fi}$ . Moreover, in order to acquire only one variable,  $P_m$  can be replaced with (13). Therefore, (25) is rewritten as:

$$J(t) = f(P_{em} | P_d, P_l, \omega) - \lambda_{fi} P_{em} \quad (26)$$

The cost function can be formed for the emissions. To achieve a thorough cost function, all of these equations are added together by the weight coefficients. (27) is the comprehensive cost function where  $w_f$ ,  $w_{hc}$ ,  $w_{co}$ , and  $w_{nox}$  are the weight coefficients that represent the importance of each part of the cost function.

$$J(t) = w_f (f(P_{em} | P_d, P_l, \omega) - \lambda_{fi} P_{em}) + w_{hc} (hc(P_{em} | P_d, P_l, \omega) - \lambda_{hci} P_{em}) + w_{co} (co(P_{em} | P_d, P_l, \omega) - \lambda_{coi} P_{em}) + w_{nox} (nox(P_{em} | P_d, P_l, \omega) - \lambda_{noxi} P_{em}) \quad (27)$$

The proper zone selection is based on the fuel curves. Therefore, the engine operation in the optimal fuel consumption area is guaranteed based on the proposed PMS. In other words, if the cost function just covers the emissions, the fuel consumption would not increase significantly. Consequently, in this paper, the values of the weight coefficients for emission reduction are assumed to be  $w_f=0$ ,  $w_{hc}=1$ ,  $w_{co}=1$  and  $w_{nox}=1$ .

In this study, two control variables ( $P_{em}$  and  $S$ ) are used to manipulate the ICE and MG.  $P_{em}$  is the power of MG in the mechanical side, and  $S$  is the binary variable that defines on or off mode of the ICE. If  $S$  equals 1, and the engine speed is more than its idle speed, then the ICE will be on. Otherwise, it will be off.

$S$  will be zero in the following situations:

- If SOC of the battery is more than  $SOC_L$  and at the same time, the MG and batteries can provide enough power for traction. In other



words, if (28) and (29) are satisfied.

$$-P_d \geq P_{em\_min} \quad (28)$$

$$\frac{-P_d}{\eta_{mm}} - P_L \geq P_{b\_min} \quad (29)$$

- In the regenerative braking mode, if the ICE is off, the kinetic energy of the wheels will be captured by MG. It is assumed that just 60% of this energy can be regenerated (Kalogirou et al., 2008).

The results should satisfy the following limits.

$$P_{em\_min}(t) \leq P_{em}(t) \leq P_{em\_max}(t) \quad \forall t \in [0, t_e] \quad (30)$$

$$P_{s\_min}(t) \leq P_s(t) \leq P_{s\_max}(t) \quad \forall t \in [0, t_e] \quad (31)$$

$$Zone_{min}(t) \leq Zone(t) \leq Zone_{max}(t) \quad \forall t \in [0, t_e] \quad (32)$$

$$SOC(t_e) \approx SOC_L \quad (33)$$

$$SOC(t) \geq SOC_L \quad \forall t \in (0, t_e) \quad (34)$$

However, the ICE can work in higher zones compared to the optimal area, if the SOC is lower than  $SOC_L$  or

when the driving cycle is missing, these constraints can be defined by design engineers.

### Online Zone Selection

The zone selection is an important section of the proposed strategy. The two variables ( $dSOC$  and  $\lambda^*$ ) are used to manipulate the zones.  $dSOC$  indicates the SOC situation such as (35) where,  $SOC_{ref}$  is reference value for the battery SOC. The zone shifting direction is determined by  $dSOC$  and time of the zone shifting is dependent on the value of  $\lambda^*$ .

$$d_{soc} = SOC - SOC_{ref} \quad (35)$$

In each loop of the program, the zone number is allowed to change just one unit. In other words, the engine operating point can jump from present zone just to the neighbor zones. For positive  $dSOC$ , it will jump to the zone with lower power. Otherwise, the zone shifting direction will be towards the neighbor zone that has higher power points.

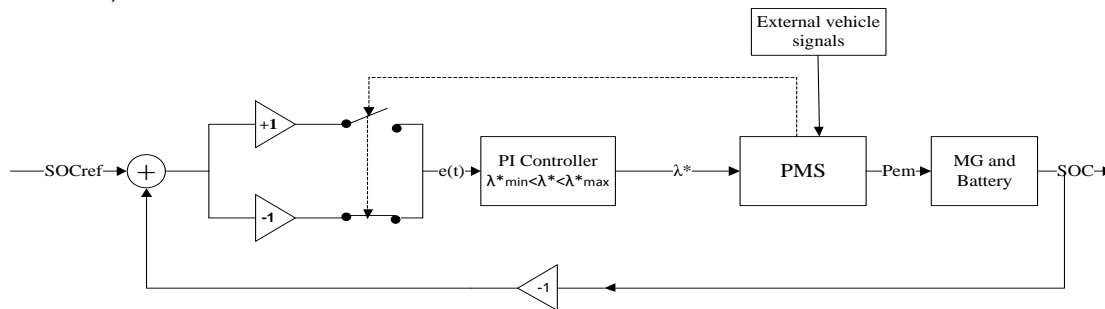


FIG. 9 FEEDBACK DIAGRAM FOR ESTIMATING  $\lambda^*$

The  $\lambda^*$  is the online calculated parameter to select the appropriate zone for the engine operating point. The zone shifting occurs when the slope of the neighbor zone is closer to the  $\lambda^*$  than the present zone slope. The  $\lambda^*$  is calculated by a system shown in Fig. 9. There is a limitation for  $\lambda^*$  which depends on the characteristics of the engine map. The  $\lambda^*$  is a comparative parameter between the slope of the neighbor zones. Therefore, the lower and upper constraints of the  $\lambda^*$  are the minimum and maximum members of the fuel slope lookup table, respectively.

The input signal of the proportional integrator (PI) controller is multiplied by -1, if the slope of the neighbor zones has reduced with the increasing power. Otherwise, the multiplier is +1. So, the  $\lambda^*$  is equal to

$$\lambda^* = \lambda_0 + K_P e(t) + K_I \int_0^t e(v) dv \quad (36)$$

where  $\lambda_0$  is an initial guess,  $e(t)$  is the input of the PI

controller. Selection of the parameters  $K_P$  and  $K_I$  for a small closed-loop bandwidth allows tracking the  $SOC_{ref}$  by means of the actual SOC (Kalogirou et al., 2008).

The proper initial value for  $\lambda^*$  ( $\lambda_0$ ) is the slope of the most optimum zone. With this selection, the engine operates near the efficient zone at the start of the trip. Appropriately, tuning of the parameters  $K_P$  and  $K_I$  is described and analyzed in (Kessels et al., 2007). The considered values for  $\lambda_0$ ,  $K_P$  and  $K_I$  are  $25 \times 10^{-7}$ ,  $67 \times 10^{-8}$ , and  $33 \times 10^{-5}$ , respectively.

The  $SOC_{ref}$  has an essential role in choosing the proper zone. The DP SOC trajectory for the predictive driving cycle is assumed to be an appropriate trajectory for SOC, therefore, in the literatures the DP is used as a comparative method (Yang et al., 2010; Gong et al., 2007; Kessels et al., 2008). However, this method is time consuming and has heavy numerical calculations.

Therefore, an easy and practical  $SOC_{ref}$  is suggested. The  $SOC_{ref}$  is considered as a straight line from  $SOC_H$  at the beginning of the trip to  $SOC_L$  at the end. However, if the battery SOC reaches  $SOC_L$  before the end of the trip, then the  $SOC_{ref}$  will be switched to the horizontal line of the  $SOC_L$  value. These two situations are shown in Fig. 10 and Fig. 11.

$SOC_{ref}$  is a reference and guide to manipulate the zones and to calculate  $\lambda^*$ . Hence, in some low speed urban areas, the engine is usually off. Therefore, the MG provides the traction power for most of the time. Consequently, SOC will be lower than  $SOC_{ref}$  in the CD (charge depletion) mode such as shown in Fig. 10.

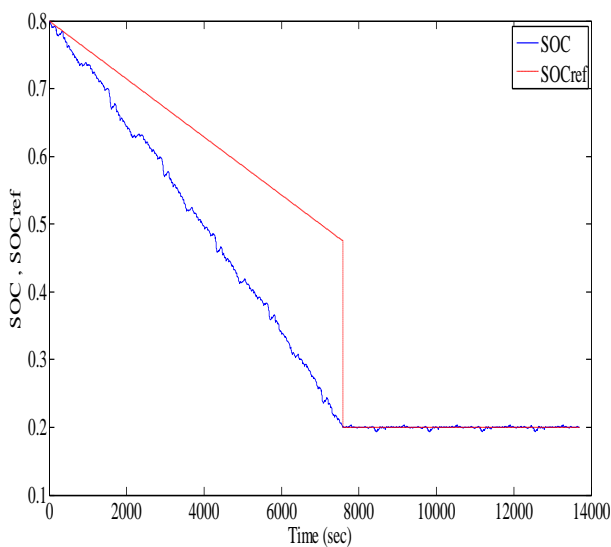


FIG. 10 SOC AND  $SOC_{REF}$  FOR 10 CYCLES OF UDDS (Alipour et al., 2012)

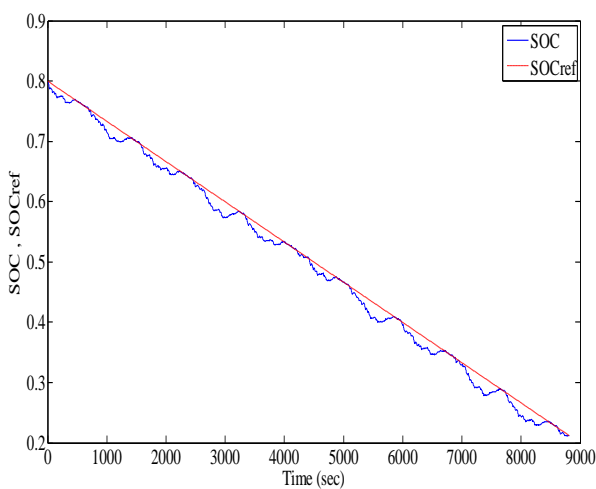


FIG. 11 SOC AND  $SOC_{REF}$  FOR 10 CYCLES OF INDIA\_HWY (Alipour et al., 2012)

Fig. 11 shows the results of 10 repetitions of the India\_HWY driving cycle, in which, speed is high;

therefore, usually the engine is on and provides most of the traction power. Hence, the battery is depleted slowly, but it should be depleted to  $SOC_L$  before the end of the trip. The  $SOC_{ref}$  is used for this goal and the length of the trip defines the slope of the  $SOC_{ref}$ . A correct trip length prediction has an important role in the battery discharging slope.

If the driver changes his destination in the middle of the trip, a new  $SOC_{ref}$  is established which is a straight line from the present SOC to  $SOC_L$  at the end of the trip. If the driver does not specify the destination, the  $SOC_{ref}$  can be a horizontal line with  $SOC_L$  value. Therefore, the engine will be off in charge depletion mode. However, this condition is not optimal.

### Online Adaptive Strategy

The proposed PMS fails to consider the driving cycle condition. However, the vehicle efficiency may be increased due to the consideration of the driving pattern. In this paper, the driving cycles are classified into two groups as urban and highway. Generally, in the highway, the power demand and the vehicle speed are high and the engine can easily work in the efficient area. However, in the urban areas the vehicle speed is low, and it stops working frequently. Furthermore, it is possible that a driver drives his vehicle in different driving patterns in one day. Therefore, it is logical that the battery can be charged in the highway and while discharged in the urban.

This idea is added to the proposed PMS by shifting the operating zone to the neighbor zone with higher power and keeping the engine on (if SOC is lower than  $SOC_{ref}$ ) in the highway driving cycles. In the urban cycles, the engine should be operated in the low power zones.

The driver can manually define the type of the driving conditions (highway or urban). However, each cycle can be divided into several small highways and urban cycles. It is assumed that the road condition ahead will be similar to the recent past condition (say 40 seconds for these durations). So, by checking the driving cycle of the past moments, the road condition is defined in the future. If the vehicle speed at all moments of a past period or the average speed of the vehicle is greater than a certain speed value, then the next period should be considered as a highway, otherwise it is considered as urban. This specific speed is acquired by trial and error. In this paper, the used specific speed is 32.4 km/h.



In this strategy,  $dsoc$  is the adapted factor. Therefore, the driver cycle mode effects the zone selection. Moreover, the battery should be charged in the highway, and be used in the urban. This online adaptive strategy can improve the fuel saving mainly in the combined driving cycles, but it may increase the emissions. In the highway driving cycles, the engine

operating points are moved rapidly towards the high power areas. Generally in these areas, the emissions are not in the optimum points. However, this subject is dependent on the engine characteristics, but it is the case in most of them.

The implementation schematic for the proposed PMS is shown in Fig. 12.

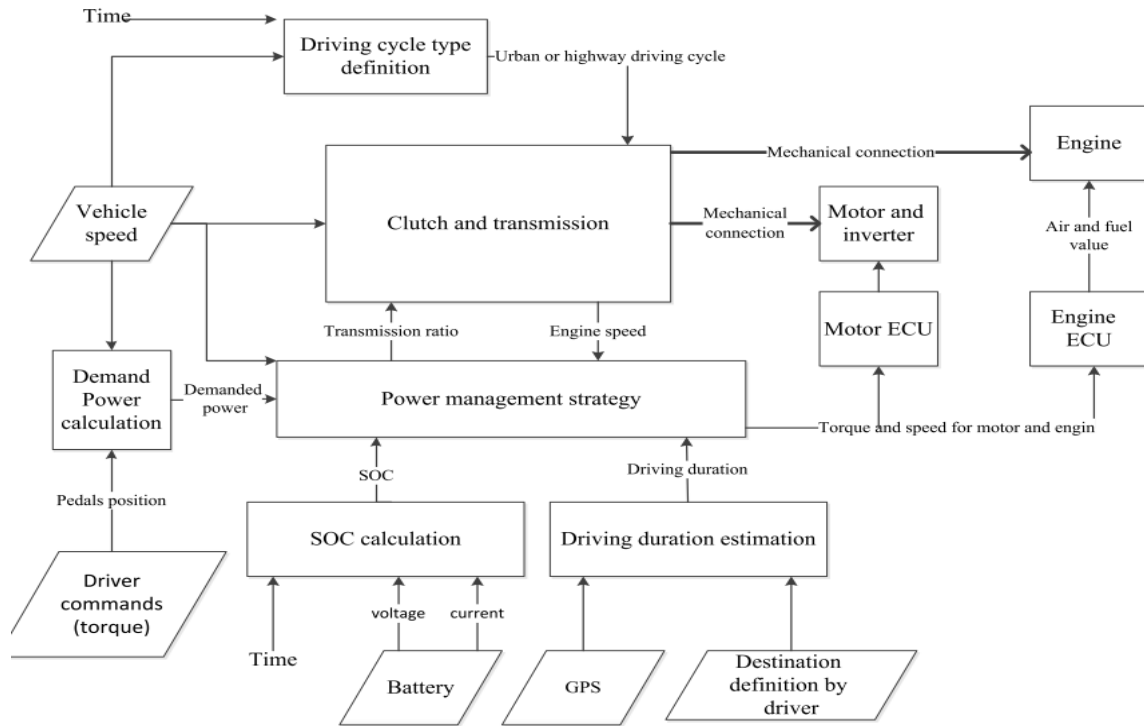


FIG. 12 THE IMPLEMENTATION SCHEMATIC FOR THE PROPOSED PMS

## Simulation Results

The proposed PMS is simulated in the ADVISOR environment for several driving cycles (Alipour et al., 2010). The results are compared with that of a heuristic rule based PMS proposed in (Banvait et al., 2009). The assumed vehicle parameters are presented in Table 1. The components of this PHEV are given in Table 2. Furthermore, another simulation is performed for this vehicle with the SI63 engine. The vehicle weight with this new engine is 1470 kgs.

The simulation is performed for five combined driving cycles and ten repeats of seven normal driving cycles. A list of these cycles is given in Table 3. The five combined driving cycles are formed by different highway and urban driving cycles. The average of the fuel consumption and emissions for these cycles is considered as a comparison criterion. However, a discussion is performed on the simulation results for ten repeats of the NEDC driving cycle.

TABLE 1 THE SIMULATED VEHICLE PARAMETERS

Quantity	Notation	Value	unit
Vehicle mass	$M$	1400	Kg
Front area	$A_d$	2.0	$m^2$
Air drag coefficient	$C_d$	0.3	–
Rolling resistance	$C_r$	0.015	–
Air density	$P$	1.2	$Kg/m^3$
Gravity	$G$	9.8	$m/s^2$
Wheel radius	$\omega_r$	0.3	$m$
Upper SOC level	$SOC_H$	0.8	–
Lower SOC level	$SOC_L$	0.2	–
Gear ratios	$g_r$	13.45_7.57_5.01_3.77_3.01	–

TABLE 2 THE SIMULATED VEHICLE COMPONENTS

Engine	SI41, with 41 kW maximum power and 0.34 peak efficiency, 1.0L, 3cylinders.
Electric machine	AC59, with 56 kW maximum power and 0.91 peak efficiency
Battery	NIMH28_OVANIC, with (C/3) 28 Ah nominal capacity and 335 V nominal voltage, 6V cell nominal voltage, 3.6kg weight, 175 Wh nominal energy (C/3), 1.6kW peak power (10s pulse)
Transmission	TX_5SPD, with 1.00 peak efficiency

TABLE 3 LIST OF THE DRIVING CYCLES

Seven normal driving cycles	Five combined driving cycles
Cyc_EUDC Cyc_FTP Cyc_HWFET Cyc_India_urban_sample Cyc_India_hwy_sample Cyc_NEDC Cyc_UDDS	(India)_hwy_urban_hwy_urban (India)_urban_hwy_hyw_urban (India)_urban_hwy_urban (India)_hwy_hwy_urban_urban UDDS_HWFET_UDDS (2cycle)

The simulations are performed for three different strategies which are the proposed PMS with and without adaptation, and the rule based strategy from (Banvait et al., 2009). The expected goals of these strategies are the fuel, fuel and emission, emission, and NO<sub>x</sub> reduction. Furthermore, the effects of the zone correction for the NO<sub>x</sub> reduction that has been introduced in Section 5 are studied. The simulation results for seven normal driving cycles are calculated. Then the average value for these cycles is computed for each condition. The average values are shown in

Table 4.

The results for the non-adaptive PMS with the fuel optimization cost function are considered as base values for comparison. The fuel consumption is increased by changing the cost function from the fuel reduction to the emission reduction.

The SI41 NO<sub>x</sub> emission characteristic is very different from the fuel usage. Consequently, the most increase in the fuel consumption is in the NO<sub>x</sub> reduction case. Particularly, the fuel consumption is increased when the engine operation area is corrected by taking into account the NO<sub>x</sub> map. However, the NO<sub>x</sub> emission will be minimized in this case. There is 2.8% less NO<sub>x</sub> emission for the non-adaptive PMS with the zone correction in comparison to the PMS without the zone correction. At the same time, it has 0.6% more fuel consumption. There are similar results for the adaptive PMS. Consequently, the zone correction method is more beneficial. Specially, with considering that the NO<sub>x</sub> reduction is the goal of the optimization.

TABLE 4 THE AVERAGE VALUES OF THE SIMULATION RESULTS FOR THE SI41 ENGINE (AVERAGE PERFORMANCES OF THE SEVEN NORMAL CYCLES)

Power Management Strategy	Fuel Usage		HC Emission		CO Emission		NO <sub>x</sub> Emission		Total Emission	
	Liter/100Km	%	g/s	%	g/s	%	g/s	%	g/s	%
Proposed PMS without adaption-with the cost function for the fuel reduction	3.57	100	0.100	100	0.275	100	0.141	100	0.516	100
Proposed PMS without adaption-with the cost function for the emission reduction	3.64	101.9	0.098	98	0.271	98.5	0.126	89.3	0.495	95.9
Proposed PMS without adaption-with the cost function for fuel and emission reduction	3.64	101.9	0.098	98	0.271	98.5	0.126	89.3	0.495	95.9
Proposed PMS without adaption-with the cost function for NO <sub>x</sub> reduction with zone correction	3.67	102.8	0.098	98	0.294	106.9	0.121	85.8	0.513	99.4
Proposed PMS without adaption-with the cost function for NO <sub>x</sub> reduction without zone correction	3.65	102.2	0.098	98	0.278	101.1	0.125	88.6	0.501	97.1
Proposed PMS with adaption-with the cost function for the fuel reduction	3.55	99.4	0.113	113	0.333	121	0.152	107.8	0.598	115.9
Proposed PMS with adaption-with the cost function for the emission reduction	3.57	100	0.111	111	0.305	110.9	0.140	99.3	0.556	107.7
Proposed PMS with adaption-with the cost function for fuel and emission reduction	3.57	100	0.111	111	0.305	110.9	0.140	99.3	0.556	107.7
Proposed PMS with adaption-with the cost function for NO <sub>x</sub> reduction with zone correction	3.64	101.9	0.109	109	0.336	122.2	0.127	90.1	0.572	110.8
Proposed PMS with adaption-with the cost function for NO <sub>x</sub> reduction without zone correction	3.61	101.1	0.111	111	0.337	122.5	0.141	100	0.589	114.1
rule based PMS from (Banvait et al., 2009)	3.70	103.6	0.096	96	0.649	236	0.142	100.7	0.887	171.9

TABLE 5 THE AVERAGE VALUES OF THE SIMULATION RESULTS FOR THE SI41 ENGINE (AVERAGE PERFORMANCES OF THE FIVE COMBINED CYCLES)

Power Management Strategy	Fuel Usage		HC Emission		CO Emission		NO <sub>x</sub> Emission		Total Emission	
	Liter/100Km	%	g/s	%	g/s	%	g/s	%	g/s	%
Proposed PMS without adaption-with the cost function for the fuel reduction	2.16	100	0.109	100	0.344	100	0.124	100	0.577	100
Proposed PMS without adaption-with the cost function for the emission reduction	2.16	100	0.105	96.3	0.303	88.1	0.108	87.1	0.516	89.4
Proposed PMS without adaption-with the cost function for NO <sub>x</sub> reduction with zone correction	2.16	100	0.105	96.3	0.339	98.5	0.103	83.1	0.547	94.8
Proposed PMS with adaption-with the cost function for the fuel reduction	2.08	96.3	0.144	132.1	0.469	136.3	0.170	137.1	0.783	135.7
Proposed PMS with adaption-with the cost function for the emission reduction	2.12	98.1	0.141	129.3	0.444	129.1	0.162	130.6	0.747	129.5
Proposed PMS with adaption-with the cost function for NO <sub>x</sub> reduction with zone correction	2.14	99.1	0.138	126.6	0.448	130.2	0.139	112.1	0.725	125.6
rule based PMS from (Banvait et al., 2009)	2.18	100.9	0.106	97.2	0.494	143.6	0.135	108.9	0.7368	127.4

TABLE 6 THE AVERAGE VALUES OF THE SIMULATION RESULTS FOR THE SI63 ENGINE (AVERAGE PERFORMANCES OF THE FIVE COMBINED CYCLES)

Power Management Strategy	Fuel Usage		HC Emission		CO Emission		NO <sub>x</sub> Emission		Total Emission	
	Liter/100Km	%	g/s	%	g/s	%	g/s	%	g/s	%
Proposed PMS without adaption-with the cost function for the fuel reduction	2.36	100	0.083	100	0.374	100	0.077	100	0.534	100
Proposed PMS without adaption-with the cost function for the emission reduction	2.34	99.2	0.083	100	0.372	99.5	0.076	98.7	0.531	99.4
Proposed PMS with adaption-with the cost function for the fuel reduction	2.28	96.6	0.102	122.9	0.495	132.4	0.103	133.8	0.7	131.1
Proposed PMS with adaption-with the cost function for the emission reduction	2.28	96.6	0.103	124.1	0.494	132.1	0.103	133.8	0.7	131.1

Table 4 shows that the adaptive strategy causes insignificant improvement in the fuel saving for the normal driving cycles. However, it is expected that

this strategy would have more advantage for the combined driving cycles. The adaptive strategy has considerable increase in the total vehicle emission. The

engine operating points for the adaptive PMS move very fast towards higher power zones in the highway periods, but these areas are improper in the emissions point of view.

The strategy to reduce the emission has the same results as the strategy with both emission and fuel optimization method. However, it has a simple cost function. Therefore, the emission cost function is a proper function to optimize the fuel and emission.

In comparison with the rule based strategy, the presented PMS has more advantages in both the emission reduction, and the fuel saving. The rule based PMS has considerable CO emission. In this strategy, the engine is operated in the high torque areas as Fig. 13. The CO emission rate is high in this district for the SI41 engine.

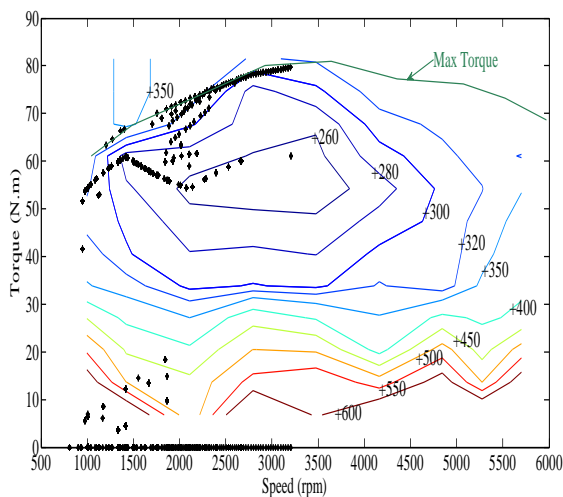


FIG. 13 ENGINE OPERATING POINTS FOR THE RULE BASED PMS IN 10 NEDC (G/KWH)

The maps for the fuel usage and NO<sub>x</sub> reduction PMSs are shown in Fig. 14 and Fig. 15, respectively. In Fig. 15, the points inside the dashed ellipses have caused the high fuel consumption for the NO<sub>x</sub> reduction mode. In fact, the defined cost function for NO<sub>x</sub> reduction strategy moves the operating points towards the low torque areas, in which the NO<sub>x</sub> emission rate is low. The NO<sub>x</sub> maps for these two situations are shown in Fig. 16 and Fig. 17. The engine operating points in Fig. 17 are closer to the low NO<sub>x</sub> emission districts than that in Fig. 16.

The mentioned methods are simulated for the combined driving cycles, for which the simulation results are calculated and then as well as the average value for each condition. The average values are shown in Table 5. The fuel consumption is reduced for the adaptive PMS. However, the other results are

similar to that of the normal driving cycles.

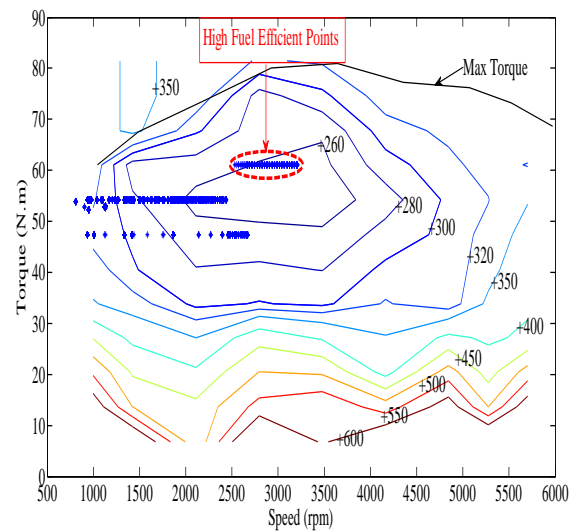


FIG. 14 THE SI41 FUEL MAP FOR THE FUEL REDUCTON COST FUNCTION IN NEDC CYCLE (G/KWH)

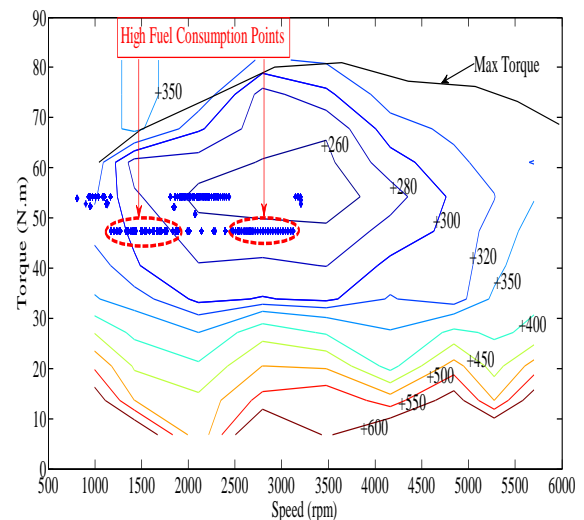


FIG. 15 THE SI41 FUEL MAP FOR THE NO<sub>x</sub> REDUCTION COST FUNCTION IN NEDC CYCLE (G/KWH)

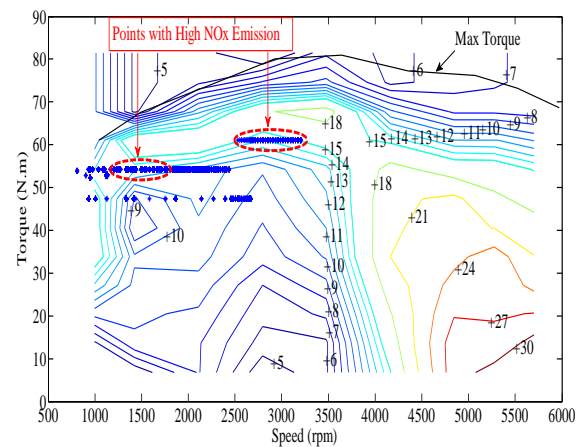


FIG. 16 THE SI41 NO<sub>x</sub> MAP FOR THE FUEL REDUCTION COST FUNCTION IN NEDC CYCLE (G/KWH)

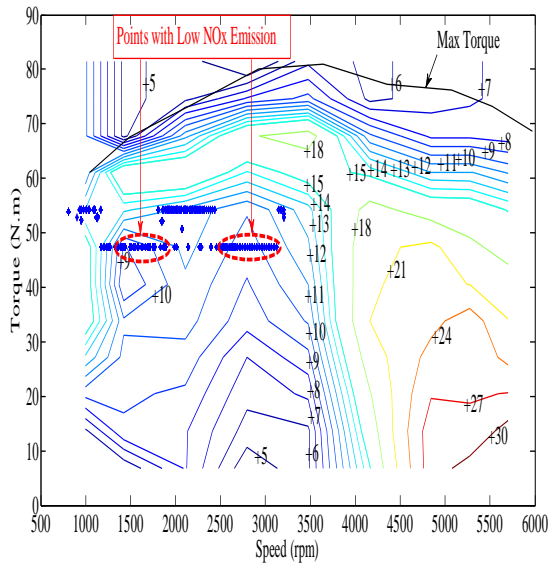


FIG. 17 THE SI41 NO<sub>x</sub> MAP FOR THE NO<sub>x</sub> REDUCTION COST FUNCTION IN NEDC CYCLE (G/KWH)

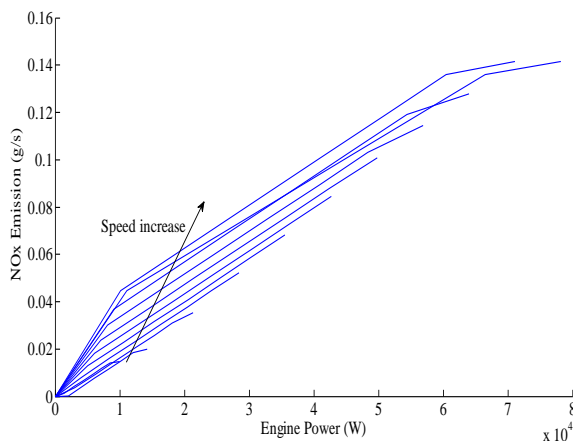


FIG. 18 NO<sub>x</sub> EMISSION MAP CHARACTERISTIC FOR THE SI63 ENGINE

Another simulation is performed for the SI63 engine. The features of this engine have some differences with the SI41 engine. For instance, the SI63 emission and fuel characteristics are almost similar together. Therefore, the zone correction for the NO<sub>x</sub> emission cannot be performed for this engine. The SI63 NO<sub>x</sub> characteristic is shown in Fig. 18. The simulation results for five combined driving cycles are calculated. Then the average value for these cycles is calculated for each condition, which is shown in Table 6. There is a considerable increase in the fuel saving and emissions for the adaptive strategy, which is in accordance with the results of the SI41 engine. However, the change in the cost function has a little change in the fuel and emission results of the SI63 engine whose characteristics are very important in the presented PMS method.

## Conclusions

This paper has presented a powerful online power management strategy for the parallel PHEVs. This PMS excludes from the need of complex mathematics as well as a priori driving cycle information. Due to these features, the proposed PMS is an applicable strategy and can reduce the emissions and the fuel consumption as well.

Furthermore, an online adaptive version of this PMS has been presented. In particular, the adaptive PMS has reduced the fuel consumption in the combined driving cycles. However, the emission has been increased in this case. Therefore, the use of the adaptive PMS is dependent on the environmental laws.

The engine characteristics have an important role in the performance of this PMS. In fact, this PMS has been established based on the engine characteristics. Therefore, the emission and the fuel consumption reduction have varying intensity for different engines. However, these effects are almost similar.

## REFERENCES

- Abdul-Hak, M., Al-Holou, N., "ITS Based Predictive Intelligent Battery Management System for Plug-in Hybrid and Electric vehicles," IEEE Vehicle Power and Propulsion Conference, 138-144, 2009.
- Alipour, H., Asaei, B., "An Online Adaptive Power Management Strategy for Plug-in Hybrid Electric Vehicles," Canadian Journal on Electrical and Electronics Engineering, 3, 3, 108-114, March 2012.
- Banvait, H., Anwar, S., Yaobin, C., "A Rule-Based Energy Management Strategy for Plug-in Hybrid Electric Vehicle (PHEV)," American Control Conference, 3938-3943, 2009.
- Bayindir, K. Ç., Gözükcük, M. A., Teke, A., "A Comprehensive Overview of Hybrid Electric Vehicle: Powertrain configurations, powertrain Control Techniques and Electronic Control Units," Energy Conversion and Management, 52, 1305-1313, 2011.
- Chen Zheng, Mi, C.C., "An Adaptive Online Energy Management Controller for Power-Split HEV Based on Dynamic Programming and Fuzzy Logic," Vehicle Power and Propulsion Conference, 2009. 335-339, 2009.
- Fajri, P., Asaei, B., "Plug-in Hybrid Conversion of a Series Hybrid Electric Vehicle and Simulation Comparison," 11th International Conference on Optimization of

- Electrical and Electronic Equipment, 287-292, 2008.
- Gao, Y., Ehsani, M., "Design and Control Methodology of Plug-in Hybrid Electric Vehicles," IEEE Trans Industrial Electronics, 57, 2, 633-640, 2010.
- Gong, Q., Li, Y., Peng, Z. R., "Computationally Efficient Optimal Power Management for Plug-in Hybrid Electric Vehicles Based on Spatial-Domain Two-Scale Dynamic Programming," IEEE International Conference on Vehicular Electronics and Safety, 90-95, 2008.
- Gong, Q., Li, Y., Peng, Z., "Power Management of Plug-in Hybrid Electric Vehicles Using Neural Network Based Trip Modeling," American Control Conference, 4601-4606, 2009.
- Gong, Q., Li, Y., Peng, Z. R., "Trip Based Power Management of Plug-in Hybrid Electric Vehicle with Two-Scale Dynamic Programming," IEEE Vehicle Power and Propulsion Conference, 12-19, 2007.
- Gong, Q., Li, Y., Peng, Z. R., "Trip-Based Optimal Power Management of Plug-in Hybrid Electric Vehicles," IEEE Trans Vehicular Technology, 57, 6, 3393-3401, 2008.
- Gong, Q., Li, Y., Peng, Z. R., "Optimal Power Management of Plug-in HEV with Intelligent Transportation System," International Conference on Advanced Intelligent mechatronics, 1-6, 2007.
- Gurkaynak, Y., Khaligh, A., "Control and Power Management of a Grid Connected Residential Photovoltaic System with Plug-in Hybrid Electric Vehicle (PHEV) Load," Applied Power Electronics Conference and Exposition, 2086-2091, 2009.
- Hui, X., Yunbo, D., "The study of Plug-In Hybrid Electric Vehicle Power Management Strategy Simulation," Vehicle Power and Propulsion Conference, 1-3, 2008.
- Kalogirou, S., Chondros, T.G., Dimarogonas, A.D., "Development of an Artificial Neural Network Based Fault Diagnostic System of an Electric Car," SAE SP-1507 Design and Technologies for Automotive Safety – Critical Systems, 61-68, 2000.
- Katrasnik, T. "Hybridization of Powertrain and Downsizing of IC Engine – A Way to Reduce Fuel Consumption and Pollutant Emissions – Part 1". Energy Conversion and Management, 48, 1411-1423, 2007.
- Kessels, J. T. B. A., Koot, M. W. T., Van Den Bosch, P. P. J., Kok, D. B., "Online Energy Management for Hybrid Electric Vehicles," IEEE Trans Vehicular Technology, 57, 6, 3428-3440, 2008.
- Kessels, J. T. B. A., "Energy Management for Automotive Power Nets," Ph.D. dissertation, Dept. Elect. Eng. Technische Univ. Eindhoven, Eindhoven, Netherlands, 2007.
- Koot, M., A. Kessels, J. T. B., de Jager, B., Heemels, W. P. M. H., van den Bosch, P. P. J., Steinbuch, M., "Energy Management Strategies for Vehicular Electric Power Systems," IEEE Trans Vehicular Technology, 54, 3, 771-782, 2005.
- Li Yushan, Zeng Qingliang, Wang Chenglong, Li Yuanjie, "Research on Fuzzy Logic Control Strategy for a Plug-in Hybrid Electric City Public Bus," International Conference on Measuring Technology and Mechatronics Automation (ICMTMA), 88-91, 2010.
- Mapelli, F., Mauri, M., Tarsitano, D. "Energy Control Strategies Comparison for a City Car Plug-In HEV," Industrial Electronics 35th Annual Conference of IEEE, 3729-3734, 2009.
- Markel, T., Brooker, A., Hendricks, T., Johnson, V., Kelly, K., Kramer, B., O'Keefe, M., Sprik, S., Wipke, K., "ADVISOR: a Systems Analysis Tool for Advanced Vehicle Modeling," Journal of Power Sources, 110, 255-266, 2002.
- Moura, S. J., Fathy, H. K., Callaway, D. S., Stein, J. L., "A Stochastic Optimal Control Approach for Power Management in Plug-In Hybrid Electric Vehicles," IEEE Trans on Control Systems Technology, 19, 3, 545-555, 2011.
- Romm, J. J., Frank, A., "Hybrid Vehicles Gain Traction," Sci. Amer, 294, 4, 72-79, 2006.
- Sciarretta, A., Guzzella, L., "Control of Hybrid Electric Vehicles, IEEE Control Systems Magazine," 27, 2, 60-70, 2007.
- Shams-Zahraei, M., Kouzani, A. Z., "A Study on Plug-in Hybrid Electric Vehicles," TENCON IEEE Region 10 Conference, 1-5, 2009.
- Shen, C., Chaoying, X., "Optimal Power Split in a Hybrid Electric Vehicle Using Improved Dynamic Programming," Power and Energy Engineering Conference (APPEEC), 1-4, 2010.
- Stockar, S., Marano, V., Rizzoni, G., Guzzella, L., "Optimal Control for Plug-in Hybrid Electric Vehicle applications,"



American Control Conference, 5024-5030, 2010.

Tulpule, P., Marano, V., Rizzoni, G., "Effects of Different PHEV Control Strategies on Vehicle Performance," American Control Conference, 3950-3955, 2009.

Wirasingha, S. G., Emadi, A., "Classification and Review of Control Strategies for Plug-In Hybrid Electric Vehicles," IEEE Trans Vehicular Technology, 60, 1, 111- 122, 2011.

Xiong, W., Zhang, Y., Yin, C., "Optimal Energy Management for a Series-Parallel Hybrid Electric Bus," Energy Conversion and Management, 50, 1730-1738, 2009.

Yang, C., Li, J., Sun, W., Zhang, B., Gao, Y., Yin, X., "Study on Global Optimization of Plug-In Hybrid Electric Vehicle Energy Management Strategies," Power and Energy Engineering Conference (APPEEC), 1-5, 2010.

Yu-shan Li, Qing-liang Zeng, Cheng-long Wang, Liang Wang, "Research on Control Strategy for Regenerative Braking of a Plug-In Hybrid Electric City Public Bus," International Conference on Intelligent Computation Technology and Automation, 842-845, 2009.

Zhang, C., Vahidi, A., Pisu, P., Li, X., Tennant, K., "Role of Terrain Preview in Energy Management of Hybrid Electric Vehicles," IEEE Trans Vehicular Technology, 59, 3, 1139-1147, 2010.

Zhang, C., Vahid, A., "Real-Time Optimal Control of Plug-in Hybrid Vehicles with Trip Preview," American Control

Conference, 6917-6922, 2010.



**Hasan Alipour** was born in Tabriz, Iran in 1985. He received B.Sc. degree in Electrical Engineering from Iran University of Science and Technology, Iran, in 2008; M.Sc. degree in Power Electrical Engineering from the University of Tehran, Iran, 2011. Currently, he is a Ph.D. Student in the University of Tabriz, Iran.

His research interests include all fields in electric and hybrid electric vehicles such as: electric vehicle stability control, hybrid electric power management strategies, and other control application in HEVs and EVs.



**Behzad Asaei** received the B.Sc. and M.Sc. degrees from the University of Tehran, Tehran, Iran, in 1988 and 1990, respectively, and the Ph.D. degree from the Sydney University, NSW, Australia, in 1995, all in electrical engineering.

Since 2006, he has been the Director of the Energy and Automotive Technology Laboratory, School of Electrical and Computer Engineering, University of Tehran. His research interests include the field of automotive electronics, solar energy, electric and hybrid electric vehicles, power electronics, and motor drives in which several projects including two electric vehicles, hybrid electric locomotive, solar car, hybrid motorcycle, electric bike, and automotive electronics have been completed.